Analytic Solutions of Von Kármán Plate under Arbitrary Uniform Pressure Part I: Equations in Differential Form

Xiaoxu Zhong [3], Shijun Liao [1,2,3] *

[1] State Key Laboratory of Ocean Engineering, Shanghai 200240, China
[2] Collaborative Innovative Center for Advanced Ship and Deep-Sea Exploration, Shanghai 200240, China
[3] School of Naval Architecture, Ocean and Civil Engineering Shanghai Jiao Tong University, Shanghai 200240, China

Abstract *The large deflection of a circular plate under a uniform external pressure is a classic problem in mechanics, dated back to Von Kármán [1]. In this paper, we solve this famous problem by means of the homotopy analysis method (HAM), an analytic approximation method for highly nonlinear equations. Convergent series solutions with four kinds of boundaries are successfully obtained, with large enough ratio of central deflection to thickness $w(0)/h > 20$ that is large enough for the majority of applications. In fact, by means of this approach, accurate analytic approximations can be obtained for a circular plate with arbitrary uniform external pressure. Especially, we proved that the perturbation methods for any a perturbation quantity (including Vincent's [2] and Chien's [3] methods) and the modified iteration method [4] are only the special cases of the HAM. However, the HAM approach works well even if these perturbation methods become invalid. In addition, our results agree well with Zheng's excellent work [5]. All of these indicate the validity and potential of the HAM for the famous Von Kármán's plate equations in solid mechanics, and show the superiority of the HAM over perturbation methods.*

Key Words circular plate, arbitrary uniform external pressure, homotopy analysis method, HAM

1. Introduction

The large deflection of a circular plate under a uniform external pressure is a classic problem that has received much attention over the past century,

*Corresponding author. Email address: sjliao@sjtu.edu.cn

since it plays an important role in many engineering fields, such as mechanical and marine engineering, the precision instrument manufacture, and so on. The Kirchhoff−Love plate theory developed by Love [6] in 1888 used some assumptions proposed by Kirchhoff, which characterizes the small transverse displacement of a thin plate. Out of the assumption of small deflections, by neglecting all terms higher than quadratic in the energy expression under given forces, Love derived the linear differential equations for the equilibrium position of the shell [7]. However, this model is valid only if the transverse displacement is small, compared to the thickness of plate. To construct a theory for large displacements, Von Kármán [1] assumed that stress is linear with strain, and took the correct nonlinear relations between the in-plane strains and the displacements. In this way, he came up in 1910 with the celebrated Von Kármán's plate equations [1], which are coupled and have strong nonlinearity. The Von Kármán's plate equations in differential form describing the large deflection of a circular thin plate under a uniform external pressure are:

$$y^2 \frac{d^2\varphi(y)}{dy^2} = \varphi(y)S(y) + Qy^2, \tag{1}$$

$$y^2 \frac{d^2 S(y)}{dy^2} = -\frac{1}{2}\varphi^2(y), \qquad y \in (0,1), \tag{2}$$

subject to the boundary conditions

$$\varphi(0) = S(0) = 0, \tag{3}$$

$$\varphi(1) = \frac{\lambda}{\lambda - 1} \cdot \left.\frac{d\varphi(y)}{dy}\right|_{y=1}, \qquad S(1) = \frac{\mu}{\mu - 1} \cdot \left.\frac{dS(y)}{dy}\right|_{y=1}, \tag{4}$$

with the definitions

$$y = \frac{r^2}{R_a^2}, \quad W(y) = \sqrt{3(1-\nu^2)}\frac{w(y)}{h}, \quad \varphi(y) = y\frac{dW(y)}{dy}, \tag{5}$$

$$S(y) = 3(1-\nu^2)\frac{R_a^2 N_r}{Eh^3}y, \quad Q = \frac{3(1-\nu^2)\sqrt{3(1-\nu^2)}R_a^4}{4Eh^4}p, \tag{6}$$

where r is the radial coordinate whose origin locates at the center of the plate, E, ν, R_a, h, $w(y)$, N_r and p are Young's modulus of elasticity, the Poisson's ratio, radius, thickness, deflection, the radial membrane force of the plate and the external uniform load, respectively, λ and μ are parameters related to the boundary conditions at $y = 1$. The dimensionless central deflection

$$W(y) = -\int_y^1 \frac{1}{\varepsilon}\varphi(\varepsilon)d\varepsilon \tag{7}$$

can be derived from Eq.(5). Note that Q is a constant, dependent upon the uniform external pressure p. In this paper, we consider four kinds of boundaries:

(a) Clamped: $\lambda = 0$ and $\mu = 2/(1-\nu)$;

(b) Moveable clamped: $\lambda = 0$ and $\mu = 0$;

(c) Simple support: $\lambda = 2/(1+\nu)$ and $\mu = 0$;

(d) Simple hinged support: $\lambda = 2/(1+\nu)$ and $\mu = 2/(1-\nu)$.

Over the past century, lots of analytic approximation methods and numerical techniques are proposed [8–15] for the Von Kármán's plate equations. Especially, some perturbation methods [2–4] based on small physical parameters (called perturbation quantity) are widely used. In 1931, Vincent [2] used the load Q as a small physical parameter to solve the Von Kármán's plate equations. By means of expanding $\varphi(y)$ and $S(y)$ into a power series of the load Q:

$$\varphi(y) = \varphi^{(V)}(y) = \sum_{i=1}^{+\infty} \varphi_i^{(V)}(y) Q^{2i-1}, \tag{8}$$

$$S(y) = S^{(V)}(y) = \sum_{i=1}^{+\infty} S_i^{(V)}(y) Q^{2i}, \tag{9}$$

with the definition of the initial guess

$$S_0^{(V)}(y) = 0,$$

the procedures of Vincent's perturbation method [2] are:

$$y^2 \frac{d^2\varphi_m^{(V)}(y)}{dy^2} = \sum_{i=1}^{m} \varphi_i^{(V)}(y) S_{m-i}^{(V)}(y) + (1-\chi_m)y^2, \tag{10}$$

$$y^2 \frac{d^2 S_m^{(V)}(y)}{dy^2} = -\frac{1}{2}\sum_{i=1}^{m} \varphi_i^{(V)}(y)\varphi_{m+1-i}^{(V)}(y), \tag{11}$$

subject to the boundary conditions

$$\varphi_m^{(V)}(0) = S_m^{(V)}(0) = 0, \tag{12}$$

$$\varphi_m^{(V)}(1) = \frac{\lambda}{\lambda - 1} \cdot \left. \frac{d\varphi_m^{(V)}(y)}{dy} \right|_{y=1}, \qquad S_m^{(V)}(1) = \frac{\mu}{\mu - 1} \cdot \left. \frac{dS_m^{(V)}(y)}{dy} \right|_{y=1}. \tag{13}$$

Unfortunately, Vincent's perturbation method [2] is valid only for a rather small ratio of central deflection to plate thickness $w(0)/h < 0.52$ for a circular plate with clamped boundary [16]. Thereafter, extensive researches regarding the selection of a proper perturbation quantity were done. For example, Chien [3], Chien and Yeh [17], and Hu [18] took different physical parameters such as the central deflection and the average angular deflection as the perturbation quantity to solve this problem. In order to find out which physical parameter is the most suitable as the perturbation quantity, Chen and Kuang [16] compared the results given by the different perturbation quantities and got the conclusion that the central deflection is the best, which gives convergent results within $w(0)/h < 2.44$ for a circular plate with clamped boundary. Thus, it is reasonable to expand the load Q into the series of $W(0)$, because the corresponding Q increases sharply as $W(0)$ enlarges. Therefore, $W(0)$ is more appropriate than Q, and it makes sense to introduce the $W(0)$ into Von Kármán's plate equations to enlarge the convergent region. Procedures of Chien's perturbation method [3] using the central deflection as the perturbation quantity are as follows

$$\varphi(y) = \varphi^{(C)}(y) = \sum_{m=1}^{+\infty} \varphi_m^{(C)}(y) W^{2m-1}(0), \tag{14}$$

$$S(y) = S^{(C)}(y) = \sum_{m=1}^{+\infty} S_m^{(C)}(y) W^{2m}(0), \tag{15}$$

$$Q = Q^{(C)} = \sum_{m=1}^{+\infty} Q_m^{(C)} W^{2m-1}(0), \tag{16}$$

where $\varphi_m^{(C)}(y)$ and $S_m^{(C)}(y)$ are governed by

$$y^2 \frac{d^2\varphi_m^{(C)}(y)}{dy^2} = \sum_{i=1}^{m} \varphi_i^{(C)}(y) S_{m-i}^{(C)}(y) + Q_m^{(C)} \cdot y^2, \tag{17}$$

$$y^2 \frac{d^2 S_m^{(C)}(y)}{dy^2} = -\frac{1}{2} \sum_{i=1}^{m} \varphi_i^{(C)}(y) \varphi_{m+1-i}^{(C)}(y), \tag{18}$$

subject to the boundary conditions

$$\varphi_m^{(C)}(0) = S_m^{(C)}(0) = 0, \tag{19}$$

$$\varphi_m^{(C)}(1) = \frac{\lambda}{\lambda - 1} \cdot \left. \frac{d\varphi_m^{(C)}(y)}{dy} \right|_{y=1}, \qquad S_m^{(C)}(1) = \frac{\mu}{\mu - 1} \cdot \left. \frac{dS_m^{(C)}(y)}{dy} \right|_{y=1}, \tag{20}$$

with the restriction condition

$$-\int_0^1 \frac{1}{\varepsilon} \cdot \varphi_m^{(C)}(\varepsilon) d\varepsilon = (1 - \chi_m) \tag{21}$$

for $Q_m^{(C)}$ and the definition of the initial guess

$$S_0^{(C)}(y) = 0,$$

and the definition of χ_m in (21):

$$\chi_m = \begin{cases} 1 & \text{when } m = 1, \\ 0 & \text{when } m \geq 2. \end{cases} \tag{22}$$

It is a pity that, as pointed out by Volmir [19], the deformation curve given by the Chien's perturbation method [3] becomes concave at centre when the central deformation increases to a certain level. This is obviously in contradiction with physical phenomena. In summary, the perturbation methods [2, 3] for a circular plate are valid only for small physical parameters.

In 1965, a modified iteration method was presented by Yeh and Liu [4] to solve the stability of a shell and the large deflection of circular plate, which inherits the merits of Chien's perturbation method [3] and iteration technique. Using this approach, the iterative process becomes clear and simple, and the problems of plate and shell are, therefore, convenient to be solved. Their iteration procedures [4] are as follows:

$$y^2 \frac{d^2\psi_n(y)}{dy^2} = -\frac{1}{2}\vartheta_n^2(y), \qquad y \in (0, 1), \tag{23}$$

$$y^2 \frac{d^2\vartheta_{n+1}(y)}{dy^2} = \vartheta_n(y)\psi_n(y) + Q_n y^2, \tag{24}$$

subject to the boundary conditions:

$$\vartheta_{n+1}(0) = \psi_n(0) = 0, \tag{25}$$

$$\vartheta_{n+1}(1) = \frac{\lambda}{\lambda-1}\cdot\left.\frac{d\vartheta_{n+1}(y)}{dy}\right|_{y=1}, \quad \psi_n(1) = \frac{\mu}{\mu-1}\cdot\left.\frac{d\psi_n(y)}{dy}\right|_{y=1}, \tag{26}$$

with the restriction condition for Q_n:

$$W(0) = a = -\int_0^1 \frac{1}{\varepsilon}\vartheta_{n+1}(\varepsilon)d\varepsilon \tag{27}$$

and the definition of the initial guess

$$\vartheta_1(y) = \frac{-2a}{2\lambda+1}[(\lambda+1)y - y^2]. \tag{28}$$

In 1989, the relationship between Chien's perturbation solutions [3] and the modified iterative solutions [4] was studied by Zhou [20], who found that they have the same convergent region. Therefore, even the modified iterative method [4] is valid only for a small central deflection, too. According to Zhou's work [20], iteration itself can not enlarge the convergence radius of perturbation series, although it can greatly enhance the computational efficiency.

In 1958, an iterative technique was presented by Keller and Reiss [21] for a thin circular plate under a uniform lateral pressure. It was found that, with a simple iterative technique, they gained convergent results only in a limited range of the load that is used as the perturbation quantity. Physically, it is the amplification of the so-called "normal force" at each step of iteration that leads to the divergence of the stresses and displacements. In order to remedy the discrepancy, Keller and Reiss [21] introduced an interpolation parameter to their iteration procedure. Fortunately, the interpolation iterative method yields convergent solutions for loads as large as $Q = 7000$. However, Keller and Reiss [21] did not prove the convergence of the interpolated iteration scheme for arbitrary values of load. Moreover, while all of the iterations can be obtained explicitly as polynomials, their degrees increase geometrically. Consequently the iterations rapidly become unwieldy and unpractical for numerical tabulation. Therefore, Keller and Reiss [21] computed the iterations approximately by means of finite differences and gave the numerical results.

The above-mentioned methods largely enrich the approaches for the Von Kármán's plate equations. However, they do not give answers to the convergence of solutions. In 1988, the convergent solutions of Von Kármán's plate equations were obtained by Zheng and Zhou [22] using the interpolation iterative method. Especially, they successfully *proved* that solution series given by the interpolation iterative method are convergent for arbitrary values of load if proper interpolation iterative parameter is chosen [22]. Zheng and Zhou's work [22] is indeed a milestone about the Von Kármán's plate equations.

In addition, many numerical methods, such as the finite element method [23] and the boundary element methods [24], were used to solve the Von Kármán's plate equations. However, numerical error increases rapidly as the central deflection increases, therefore these numerical methods are no longer valid when deflection becomes large. In 2015, a wavelet method [25, 26] was proposed to solve large deflection of circular plates, which can guarantee both of the approximation accuracy and the computational efficiency.

In this paper the large deflection of a circular plate under a uniform external pressure is solved by means of an analytic technique for highly nonlinear problems, namely, the homotopy analysis method (HAM) [27–33], which was proposed by Liao [27] in 1992. Unlike perturbation technique, the HAM is independent of any small/large physical parameters. Besides, unlike other analytic techniques, the HAM provides a simple way to guarantee the convergence of solution series by means of introducing the so-called "convergence-control parameter". In addition, the HAM provides us great freedom to choose equation-type and solution expression of the high-order linear equations. As a powerful technique to solve highly nonlinear equations, the HAM was successfully employed to solve various types of nonlinear problems over the past two decades [34–44]. Especially, as shown in [45–49], the HAM can bring us something completely new/different: the steady-state resonant waves were first predicted by the HAM in theory and then confirmed experimentally in a lab [47]. So, the HAM should provide us a suitable analytic approach for Von Kármán's plate equations, too. In Part (I), we first take Von Kármán's plate equations in the differential form with the clamped boundary as an example, and obtain the convergent analytic results in the case of $w(0)/h = 4.24$ by means of the HAM (without iteration), which is larger than the maximum convergence range ($w(0)/h < 2.44$) of the perturbation method [16]. Further, the HAM−based iteration approach is presented to gain convergent solutions within a large enough ratio of $w(0)/h > 20$. Our results given by the HAM−based iteration approach agree very well with those given by Zheng's [5]. Furthermore, convergent solutions of the Von Kármán's plate equations with other three boundaries (moveable clamped, simple support and simple hinged support) are presented. Finally, we prove that the perturbation methods for any a perturbation quantity (including

Vincent's [2] and Chien's [3] perturbation methods) and the modified iteration method [4] are only special cases of the HAM. In Part (II), two HAM-based approaches are proposed to solve the Von Kármán's plate equations in the integral form for arbitrary uniform pressure, and it is proved that the interpolation iterative method [21] is only a special case of the HAM, too.

2. Analytic approach based on the HAM

According to Zheng [5], $\varphi(y)$ and $S(y)$ are power series in y. Therefore, we express $\varphi(y)$ and $S(y)$ in power series

$$\varphi(y) = \sum_{m=1}^{+\infty} a_m \cdot y^m, \quad S(y) = \sum_{m=1}^{+\infty} b_m \cdot y^m, \tag{29}$$

where a_m and b_m are constant coefficients to be determined. They provide us the so-called "solution expression" of $\varphi(y)$ and $S(y)$ in the frame of the HAM. Given

$$W(0) = a, \tag{30}$$

we have due to Eq.(7) an algebraic equation for the corresponding unknown value of Q:

$$\int_0^1 \frac{1}{\varepsilon}\varphi(\varepsilon)d\varepsilon = -a. \tag{31}$$

Let $\varphi_0(y)$ and $S_0(y)$ be initial guesses of $\varphi(y)$ and $S(y)$, respectively, which satisfy the boundary conditions (3), (4) and (31). Moreover, let $\mathcal{L}$ denote an auxiliary linear operator with property $\mathcal{L}[0] = 0$, $H_1(y)$ and $H_2(y)$ the auxiliary functions, c_0 a non-zero auxiliary parameter, called the convergence-control parameter, and $q \in [0, 1]$ the embedding parameter, respectively. Then, we construct a family of differential equations in $q \in [0, 1]$:

$$(1-q)\mathcal{L}[\Phi(y;q) - \varphi_0(y)] = c_0 q H_1(y)\mathcal{N}_1(y;q), \tag{32}$$

$$(1-q)\mathcal{L}[\Xi(y;q) - S_0(y)] = c_0 q H_2(y)\mathcal{N}_2(y;q), \tag{33}$$

subject to the boundary conditions

$$\Phi(0;q) = \Xi(0;q) = 0, \tag{34}$$

$$\Phi(1;q) = \frac{\lambda}{\lambda-1} \cdot \left.\frac{\partial\Phi(y;q)}{\partial y}\right|_{y=1}, \quad \Xi(1;q) = \frac{\mu}{\mu-1} \cdot \left.\frac{\partial\Xi(y;q)}{\partial y}\right|_{y=1}, \tag{35}$$

with the restriction condition

$$\int_0^1 \frac{1}{\varepsilon}\Phi(\varepsilon;q)d\varepsilon = -a, \tag{36}$$

where

$$\mathcal{N}_1(y;q) = y^2\frac{\partial^2\Phi(y;q)}{\partial y^2} - \Phi(y;q)\Xi(y;q) - \Theta(q)y^2, \tag{37}$$

$$\mathcal{N}_2(y;q) = y^2\frac{\partial^2\Xi(y;q)}{\partial y^2} + \frac{1}{2}\Phi^2(y;q) \tag{38}$$

are two nonlinear operators. Here we rewrite the unknown Q (for a given a) in a power series:

$$\Theta(q) = \sum_{m=0}^{+\infty} Q_m\, q^m,$$

where Q_m is determined by the algebraic equation (36).

When $q = 0$, due to the property $\mathcal{L}(0) = 0$, Eqs.(32)-(36) have the solution:

$$\Phi(y;0) = \varphi_0(y), \quad \Xi(y;0) = S_0(y). \tag{39}$$

When $q = 1$, they are equivalent to the original equations (1)-(4) and (31), provided

$$\Phi(y;1) = \varphi(y), \quad \Xi(y;1) = S(y), \quad \Theta(1) = Q. \tag{40}$$

Write

$$\Theta(0) = Q_0, \tag{41}$$

where Q_0 denotes the initial guess of Q. Therefore, as q increases from 0 to 1, $\Phi(y;q)$ varies continuously from the initial guess $\varphi_0(y)$ to $\varphi(y)$, so do $\Xi(y;q)$ from the initial guess $S_0(y)$ to $S(y)$, and $\Theta(q)$ from the initial guess Q_0 to Q, respectively. In topology, these kinds of continuous variation are called deformation. Eqs.(32)-(36) constructing the homotopies $\Phi(y;q)$, $\Xi(y;q)$ and $\Theta(q)$ are called the zeroth$-$order deformation equations.

Expanding $\Phi(y;q)$, $\Xi(y;q)$ and $\Theta(q)$ into Taylor series with respect to the embedding parameter q, we have the so-called homotopy-series:

$$\Phi(y;q) = \varphi_0(y) + \sum_{m=1}^{+\infty} \varphi_m(y)\, q^m, \tag{42}$$

$$\Xi(y;q) = S_0(y) + \sum_{m=1}^{+\infty} S_m(y)\, q^m, \tag{43}$$

$$\Theta(q) = Q_0 + \sum_{m=1}^{+\infty} Q_m\, q^m. \tag{44}$$

where

$$\varphi_m(y) = \mathcal{D}_m[\Phi(y;q)], \tag{45}$$

$$S_m(y) = \mathcal{D}_m[\Xi(y;q)], \tag{46}$$

$$Q_m = D_m[\Theta(q)], \tag{47}$$

in which

$$\mathcal{D}_m[f] = \frac{1}{m!}\frac{\partial^m f}{\partial q^m}\bigg|_{q=0} \tag{48}$$

is called the mth-order homotopy-derivative of f.

Note that the radius of convergence of a power series is finite in general. Fortunately, in the frame of the HAM, apart from the great freedom to choose the auxiliary linear operator $\mathcal{L}$, there is a convergence-control parameter c_0 contained in the homotopy-series (42)-(44). Assume that $\mathcal{L}$ and c_0 are so properly chosen that the homotopy-series (42)-(44) are convergent at $q = 1$. Then according to Eq. (40), the so-called homotopy-series solutions read:

$$\varphi(y) = \varphi_0(y) + \sum_{m=1}^{+\infty} \varphi_m(y), \tag{49}$$

$$S(y) = S_0(y) + \sum_{m=1}^{+\infty} S_m(y), \tag{50}$$

$$Q = Q_0 + \sum_{m=1}^{+\infty} Q_m. \tag{51}$$

In addition, the governing equations and boundary conditions of $\varphi_m(y)$, $S_m(y)$ and Q_m can be derived by substituting the series (42)-(44) into the zeroth-order deformation equations (32)-(36) and then equating the like-power of the embedding parameter q. The so-called mth-order deformation equations read

$$\mathcal{L}[\varphi_m(y) - \chi_m \varphi_{m-1}(y)] = c_0 H_1(y) \delta_{1,m-1}(y), \tag{52}$$

$$\mathcal{L}[S_m(y) - \chi_m S_{m-1}(y)] = c_0 H_2(y) \delta_{2,m-1}(y), \tag{53}$$

subject to the boundary conditions

$$\varphi_m(0) = S_m(0) = 0, \tag{54}$$

$$\varphi_m(1) = \frac{\lambda}{\lambda - 1} \cdot \left. \frac{\partial \varphi_m(y)}{\partial y} \right|_{y=1}, \quad S_m(1) = \frac{\mu}{\mu - 1} \cdot \left. \frac{\partial S_m(y)}{\partial y} \right|_{y=1}, \tag{55}$$

with the restriction condition for Q_{m-1}:

$$\int_0^1 \frac{1}{\varepsilon} \cdot \varphi_m(\varepsilon) d\varepsilon = 0, \tag{56}$$

where χ_m is defined by (22) and

$$\begin{aligned} \delta_{1,m-1}(y) &= \mathcal{D}_{m-1}[\mathcal{N}_1(y;q)] \\ &= y^2 \frac{\partial^2 \varphi_{m-1}(y)}{\partial y^2} - \sum_{k=0}^{m-1} \varphi_k(y) S_{m-1-k}(y) - Q_{m-1} y^2, \end{aligned} \tag{57}$$

$$\begin{aligned} \delta_{2,m-1}(y) &= \mathcal{D}_{m-1}[\mathcal{N}_2(y;q)] \\ &= y^2 \frac{\partial^2 S_{m-1}(y)}{\partial y^2} + \frac{1}{2} \sum_{k=0}^{m-1} \varphi_k(y) \varphi_{m-1-k}(y). \end{aligned} \tag{58}$$

Note that the mth-order deformation equations (52)-(56) are linear. Besides, we have great freedom to choose the auxiliary linear operator $\mathcal{L}$,the initial guesses $\varphi_0(y)$ and $S_0(y)$. According to [28], the choice of $\mathcal{L}$, $\varphi_0(y)$ and $S_0(y)$ should guarantee the solution expression (29) and the solution existence of the high-order deformation equations (52)-(56). Thus, we choose

$$\varphi_0(y) = \frac{-2a}{2\lambda + 1}[(\lambda + 1)y - y^2], \tag{59}$$

$$S_0(y) = (\mu + 1)y - y^2 \tag{60}$$

as the initial guesses of $\varphi(y)$ and $S(y)$. Since the original equations (1) and (2) are of 2nd order, it is natural to choose such a 2nd-order auxiliary linear operator

$$\mathcal{L}[u(y)] = \frac{du^2(y)}{dy^2} \tag{61}$$

with the property

$$\mathcal{L}[c_3 + c_4 y] = 0. \tag{62}$$

Considering the solution expression (29) and the property (62) of the auxiliary linear operator $\mathcal{L}$, $H_1(y)$ and $H_2(y)$ should be properly chosen so as to make sure that the right-hand side term of the high-order deformation equations (52) and (53) are in the forms:

$$c_0 H_1(y)\delta_{1,m-1}(y) = \sum_{k=0} d_{1,k}\ y^k, \tag{63}$$

$$c_0 H_2(y)\delta_{2,m-1}(y) = \sum_{k=0} d_{2,k}\ y^k, \tag{64}$$

where $d_{1,k}$ and $d_{2,k}$ are the coefficients, respectively. Therefore, the auxiliary function $H_1(y)$ and $H_2(y)$ must be in the form:

$$H_1(y) = H_2(y) = \frac{1}{y^2}. \tag{65}$$

Substituting Eqs.(61) and (65) into Eqs.(52) and (53), we have the general solutions of the high-order deformation equations (52) and (53):

$$\varphi_m(y) = \chi_m \varphi_{m-1}(y) + \int_0^y \int_0^\eta c_0 \frac{1}{\tau^2}\delta_{1,m}(\tau) d\tau d\eta + D_{1,m} y + D_{2,m}, \tag{66}$$

$$S_m(y) = \chi_k S_{m-1}(y) + \int_0^y \int_0^\eta c_0 \frac{1}{\tau^2}\delta_{2,m}(\tau) d\tau d\eta + D_{3,m} y + D_{4,m}, \tag{67}$$

where $D_{1,m}$, $D_{2,m}$, $D_{3,m}$, $D_{4,m}$ are four unknown constants, which are determined by the four linear boundary conditions (54) and (55). The unknown Q_{m-1} is given by the algebraic equation (56). As a consequence, $\varphi_m(y)$, $S_m(y)$ and Q_{m-1} of Eqs. (52) and (53) are obtained. Then, we have the nth-order approximation of $\varphi(y)$ and $S(y)$:

$$\tilde{\varphi}_n(y) = \sum_{m=0}^{n} \varphi_m(y), \tag{68}$$

$$\tilde{S}_n(y) = \sum_{m=0}^{n} S_m(y), \tag{69}$$

and the $(n-1)$th-order approximate solution of Q:

$$\tilde{Q}_{n-1} = \sum_{m=0}^{n-1} Q_m. \tag{70}$$

Define the sum of the two discrete squared residuals

$$Err = \frac{1}{K+1} \sum_{i=0}^{K} \left\{ \left[\mathcal{N}_1 \left(\frac{i}{K} \right) \right]^2 + \left[\mathcal{N}_2 \left(\frac{i}{K} \right) \right]^2 \right\}, \tag{71}$$

where $K = 100$ is used in this paper. Obviously, the smaller the Err, the more accurate the HAM approximation is.

According to Liao [28], the convergence of the homotopy-series solutions can be greatly accelerated by means of iteration technique, which uses the Mth-order homotopy-approximations

$$\check{\varphi}(y) \approx \varphi_0(y) + \sum_{m=1}^{M} \varphi_m(y), \tag{72}$$

$$\check{S}(y) \approx S_0(y) + \sum_{m=1}^{M} S_m(y) \tag{73}$$

as the new initial guesses $\varphi_0(y)$ and $S_0(y)$ for the next iteration. This provides us the Mth-order iteration of the HAM. Moreover, we neglect all higher-order terms of the right-hand side terms in Eqs. (52) and (53), say,

$$c_0 H_1(y) \cdot \delta_{1,m}(y) \approx \sum_{k=0}^{N} E_{m,k} \cdot y^k, \tag{74}$$

$$c_0 H_2(y) \cdot \delta_{2,m}(y) \approx \sum_{k=0}^{N} F_{m,k} \cdot y^k, \tag{75}$$

where $E_{m,k}$ and $F_{m,k}$ are constant coefficients, N is called the truncation order, respectively. Note that the appropriate value of the truncation order N is dependent upon the boundary condition, as shown later.

3. Result analysis

At first, the Von Kármán's plate equations with the clamped boundary are used as an example to illustrate the validity of the HAM-based approach within a quite large region of $w(0)/h$, i.e. the ratio of central deflection to thickness of the plate. Then, other three boundaries (moveable clamped, simple support and simple hinged support) are considered. Finally, we reveal that the perturbation methods for any a perturbation quantity (including Vincent's [2] and Chien's [3] perturbation methods) and the modified iteration method [4] are only special cases of the HAM. Without loss of generality, the Poisson's ratio ν is taken to be 0.3 in all cases considered in this paper.

3.1. The HAM-based approach without iteration

The HAM-based approach (without iteration) is used to solve the Von Kármán's plate equations with the clamped boundary at first. Unlike other analytic approximation methods, the HAM-based approach contains the so-called convergence-control parameter c_0, which provides us a convenient way to guarantee the convergence of the solution series. The optimal value of c_0 is determined by the minimum of Err defined by (71), i.e. the sum of the squared residual errors of the two governing equations. Take the case of $a = 5$ as an example, equivalent to $w(0)/h = 3.0$. As shown in Fig 1, the sum of the squared residuals arrives its minimum at $c_0 \approx -0.28$, which suggests that the optimal value of c_0 is about -0.28. As shown in Table 1, the sum of the squared residual errors quickly decreases to 4.9×10^{-12} by means of $c_0 = -0.28$ in the case of $a = 5$, equivalent to $w(0)/h = 3.0$. Note that the largest convergent range of the perturbation results [16] is only $w(0)/h < 2.44$. This illustrates the superiority of the HAM-based approach over the perturbation method.

In a similar way, for any a given value of a, we can always find the corresponding optimal value of c_0 for the Von Kármán's plate equations with the clamped boundary, which can be fitted by the formula:

$$c_0 = \begin{cases} -1 + 0.052a + 0.0325a^2 - 0.023a^3 + 0.0047a^4 & (0 \le a \le 4), \\ -3.892a \cdot e^{-0.845a} & (4 < a \le 7), \end{cases} \tag{76}$$

as shown in Fig.2. It should be emphasized that it is the convergence-control parameter c_0 that enables us to guarantee the convergence of the homotopy-series solutions. Therefore, the convergence-control parameter indeed plays a very important role in the frame of the HAM.

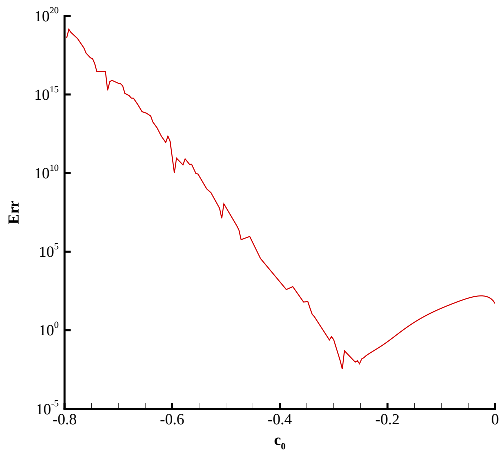

Figure 1: The sum of squared residual errors Err versus c_0 in the case of $a = 5$ for a circular plate with the clamped boundary, gained by the HAM-based approach (without iteration).

3.2. Convergence acceleration by means of iteration

Iteration can be introduced naturally into the frame of the HAM to greatly accelerate the convergence of the homotopy-series solutions. Without loss of generality, let us consider the same case of $a = 5$, equivalent to $w(0)/h = 3.0$. As shown in Fig 3, the sum of the squared residual errors arrives its minimum at $c_0 \approx -0.55$ by means of the HAM-based 1st-order iteration approach with the truncation order $N = 100$. Note that the sum of the squared residual errors quickly decreases to 1.7×10^{-24} in only 25 seconds of CPU time, which is about 50 times faster than the HAM approach without iteration, as shown in Table 1 and 2. Thus, the computational efficiency can be greatly improved by iteration. So, from the viewpoint of computational efficiency, the HAM approach with iteration is applied for other three boundaries (moveable clamped, simple support and simple hinged support) in the subsequent part of this paper.

3.3. Choice of the auxiliary parameters

To use the HAM-based iteration approach, we need choose the order M of iteration formula in (72)-(73) and the truncation order N in (74)-(75).

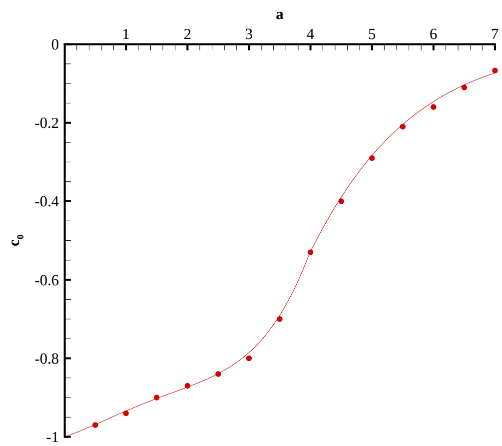

Figure 2: The optimal convergence-control parameter c_0 versus a in the case of a circular plate with the clamped boundary, in the frame of the HAM (without iteration). Symbols: optimal convergence-control parameter calculated in some cases; Solid line: fitting formula.

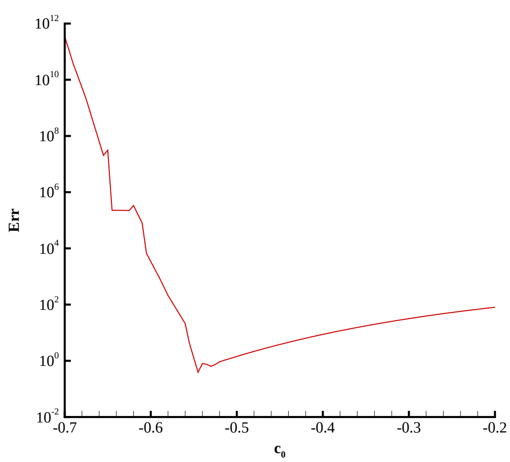

Figure 3: The sum of the squared residual errors Err versus c_0 in the case of $a = 5$ for a circular plate with the clamped boundary, given by the HAM-based 1st-order iteration approach using the truncation order $N = 100$.

Table 1: The used CPU time, the sum of the squared residual errors Err and the homotopy-approximations of Q in the case of $a = 5$ of a circular plate with the clamped boundary, given by the HAM (without iteration) using $c_0 = -0.28$.

m, order of approx.	Err	Q	CPU time (seconds)
20	6.4×10^{-2}	131.7	6
40	5.8×10^{-4}	132.1	35
60	9.3×10^{-6}	132.1	106
80	2.0×10^{-7}	132.2	243
100	5.1×10^{-9}	132.2	465
120	1.5×10^{-10}	132.2	782
140	4.9×10^{-12}	132.2	1205

Table 2: The CPU time, the sum of the squared residual errors Err and the load Q versus the iteration times in the case of $a = 5$ for a circular plate with the clamped boundary, given by the HAM-based 1st-order iteration approach using $c_0 = -0.55$ with the truncation order $N = 100$.

m, times of iteration	Err	Q	CPU time (seconds)
10	4.5×10^{-3}	132.2	5
20	4.8×10^{-11}	132.2	12
30	1.3×10^{-18}	132.2	18
40	1.7×10^{-24}	132.2	25

As shown in Fig. 4, the sum of the squared residual errors decreases to the level of 10^{-26} for the different iteration order M in the case of $a = 15$ with the clamped boundary, and the iteration order $M = 5$ corresponds to the least iteration times. The sum of the squared residual errors versus the CPU time for the different iteration order M is shown in Fig. 5. Note that the HAM-based 1st-order iteration approach ($M = 1$) corresponds to the fastest convergence, i.e. the least CPU time, mainly because a higher-order iteration needs more CPU times than the lower.

In the cases of $a = 8$ and $a = 15$ with the clamped boundary, the sum of the squared residual errors versus the CPU time given by the HAM-based 1st-order iteration approach with the different truncation order N is given in

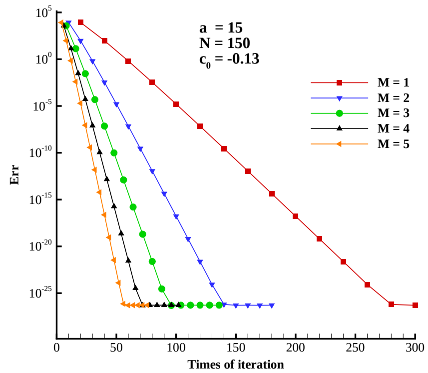

Figure 4: The sum of the squared residual errors Err versus the times of iteration in the case of $a = 15$ for a circular plate with the clamped boundary, given by the HAM-based iteration approach using $c_0 = -0.13$, the truncation order $N = 150$ and different order of iteration approach. Square: 1st-order; Triangle down: 2nd-order; Circle: 3rd-order; Triangle up: 4th-order; Triangle left: 5th-order.

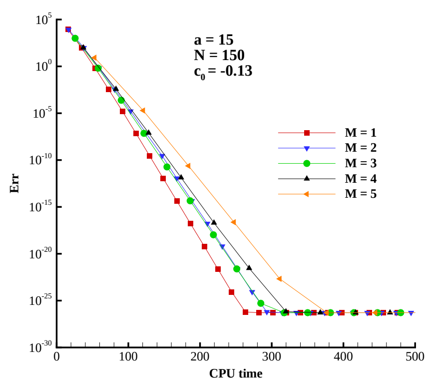

Figure 5: The sum of the squared residual errors Err versus the CPU time in the case of $a = 15$ for a circular plate with the clamped boundary, given by the HAM-based iteration approach using $c_0 = -0.13$, the truncation order $N = 150$ and different order of iteration approach. Square: 1st-order; Triangle down: 2nd-order; Circle: 3rd-order; Triangle up: 4th-order; Triangle left: 5th-order.

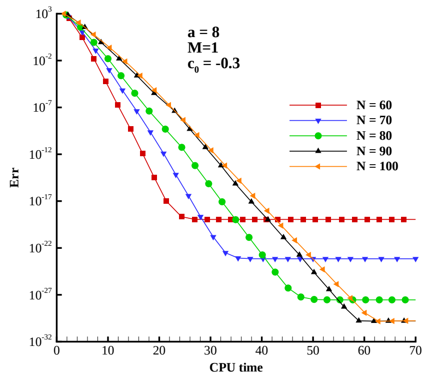

Figure 6: The sum of the squared residual errors Err versus the CPU time in the case of $a = 8$ for a circular plate with the clamped boundary, given by the HAM-based 1st-order iteration approach using $c_0 = -0.3$ and different truncation order N. Square: $N = 60$; Triangle down: $N = 70$; Circle: $N = 80$; Triangle up: $N = 90$; Triangle left: $N = 100$.

Fig. 6 and Fig. 7, respectively. The iteration converges with high accuracy as long as the truncation order N is large enough, although larger N corresponds to slower convergence.

Obviously, the nonlinearity of the Von Kármán's plate equations becomes stronger (i.e. a is larger) as the load increases. According to our computation, in the frame of the HAM-based 1st-order iteration approach, we have the following empirical formula for the truncation order:

$$N = Max\left\{100, \gamma \cdot a\right\}, \tag{77}$$

where γ is dependent upon the type of boundary:

$$\gamma = \begin{cases} 10, & clamped\ boundary, \\ 13, & moveable\ clamped\ boundary, \\ 7, & simple\ support\ boundary, \\ 5, & simple\ hinged\ support\ boundary. \end{cases}$$

For a circular plate with the clamped boundary, its optimal convergence-control parameter c_0 for the HAM-based 1st-order iteration approach can be expressed by the empirical formula:

$$c_0 = -\frac{26}{26 + a^2} \qquad (0 \le a \le 35). \tag{78}$$

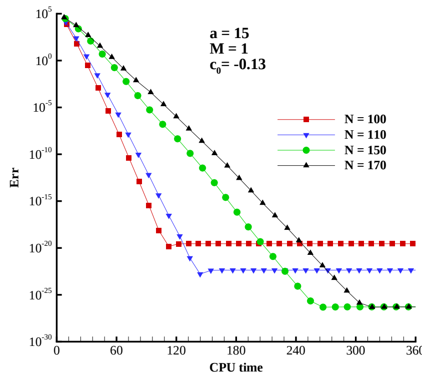

Figure 7: The sum of the squared residual errors Err versus the CPU time in the case of $a = 15$ for a circular plate with the clamped boundary, given by the HAM-based 1st-order iteration approach using $c_0 = -0.13$ and different truncation order N. Square: $N = 100$; Triangle down: $N = 110$; Circle: $N = 150$; Triangle up: $N = 170$.

For example, as shown in Table 3, the convergent analytic approximations can be obtained quickly by means of the HAM-based 1st-order iteration approach in this way, even in the case of $a = 35$, corresponding to $w(0)/h = 21.2$. As shown in Fig. 8, Chien's perturbation method [3] is valid only in the region of $w(0)/h < 2.4$, and becomes worse and worse for larger $w(0)/h$. As shown in Fig. 9, our results agree quite well with those given by Zheng [5] using the interpolation iterative method. This verifies the validity of the HAM-based iteration approach. Moreover, the convergent deflection curves under different loads even up to $pR_a^4/Eh^4 = 34632$ are shown in Fig. 10.

For a circular plate with the moveable clamped boundary, the corresponding optimal convergence-control parameter c_0 for the HAM-based 1st-order iteration approach can be expressed by the empirical formula

$$c_0 = -\frac{39}{39 + a^2} \quad (0 \le a \le 35). \tag{79}$$

For example, as shown in Table 4, the convergent accurate analytic approximations can be obtained even in the case of $a = 35$, corresponding to $w(0)/h = 21.2$. The convergent deflection curves under different loads up to $pR_a^4/Eh^4 = 5278.3$ are as shown in Fig.11.

For a circular plate with the simple support boundary, the corresponding optimal convergence-control parameter c_0 for the HAM-based 1st-order

Table 3: The convergent homotopy-approximation of the load Q in case of different values of a for a circular plate with the clamped boundary, given by the HAM-based 1st-order iteration approach with the truncation order N given by (77) and the optimal convergence-control parameter c_0 given by (78).

a	c_0	N	Q
5	-0.51	100	132.2
10	-0.21	100	957.7
15	-0.10	150	3152.1
20	-0.06	200	7386.9
25	-0.04	250	14334.1
30	-0.03	300	24665.7
35	-0.02	350	39053.6

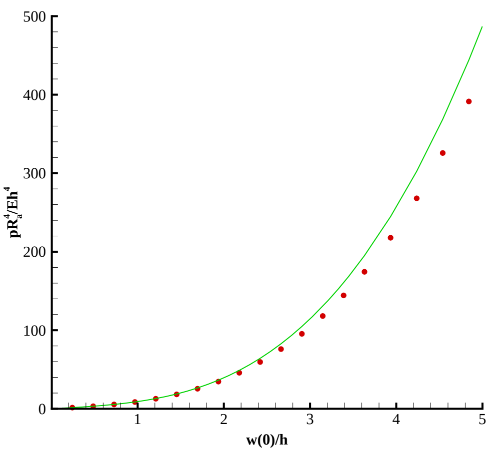

Figure 8: Comparison of the results given by the HAM-based 1st-order iteration approach and Chien's perturbation method [3] for a circular plate with the clamped boundary. Symbols: results given by Chien's perturbation method [3]; Solid line: results given by the HAM.

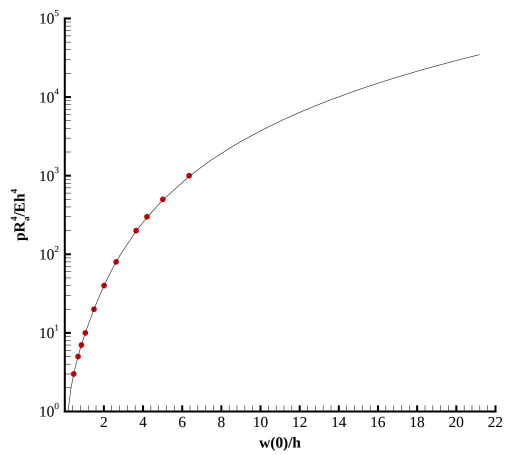

Figure 9: Comparison of the results given by the HAM-based 1st-order iteration approach and the interpolation iterative method for a circular plate with the clamped boundary. Symbols: results given by Zheng [5] using the interpolation iterative method; Solid line: results given by the HAM.

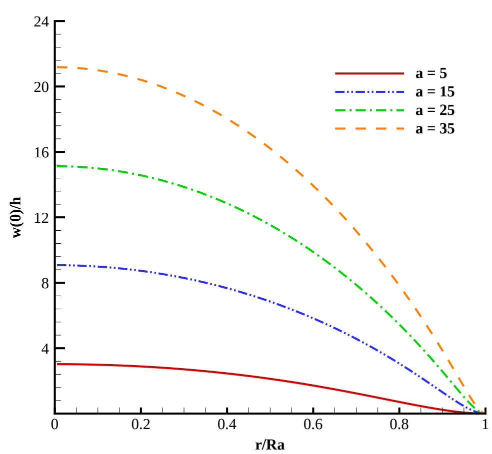

Figure 10: The deflection curves of a thin circular plate with the clamped boundary given by the HAM-based 1st-order iteration approach in the case of $a = 5, 15, 25, 35$. Solid line: $pR_a^4/Eh^4 = 117.2$; Dash-double-dotted line: $pR_a^4/Eh^4 = 2795.2$; Dash-dotted line: $pR_a^4/Eh^4 = 12711.2$; Dashed line: $pR_a^4/Eh^4 = 34632.0$.

Table 4: The convergent homotopy-approximation of the load Q in case of different values of a for a circular plate with the moveable clamped boundary, given by the HAM-based 1st-order iteration approach using the truncation order N given by (77) and the optimal convergence-control parameter c_0 given by (79).

a	c_0	N	Q
5	-0.61	100	49.3
10	-0.28	130	240.1
15	-0.15	195	657.7
20	-0.09	260	1372.5
25	-0.06	325	2450.9
30	-0.04	390	3956.8
35	-0.03	455	5952.2

iteration approach can be expressed by the empirical formula

$$c_0 = -\frac{80}{80 + a^2} \qquad (0 \le a \le 50). \tag{80}$$

For example, as shown in Table 5, the convergent analytic solutions can be obtained even in the case of $a = 50$, corresponding to $w(0)/h = 30.3$. The convergent deflection curves under different loads up to $pR_a^4/Eh^4 = 8689.9$ are as shown in Fig 12.

For a circular plate with the boundary of simple hinged support, the corresponding optimal convergence-control parameter c_0 for the HAM-based 1st-order iteration approach can be expressed by the empirical formula

$$c_0 = -\frac{40}{40 + a^{\frac{5}{2}}} \qquad (0 \le a \le 50). \tag{81}$$

For example, as shown in Table 6, the convergent analytic solutions can be obtained even in the case of $a = 50$, corresponding to $w(0)/h = 30.3$. The convergent deflection curves under different loads up to $pR_a^4/Eh^4 = 99279.8$ are shown in Fig. 13.

4. Relations between the HAM and other methods

In this section, we prove that the perturbation methods for any a perturbation quantity (including Vincent's [2] and Chien's [3] perturbation meth-

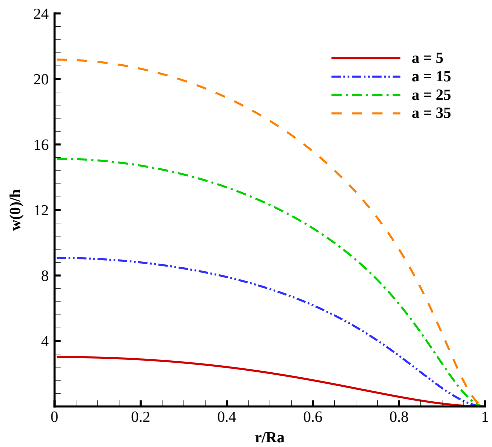

Figure 11: The deflection curves of a thin circular plate with the moveable clamped boundary given by the HAM-based 1st-order iteration approach in the case of $a = 5, 15, 25, 35$. Solid line: $pR_a^4/Eh^4 = 43.7$; Dash-double-dotted line: $pR_a^4/Eh^4 = 583.2$; Dash-dotted line: $pR_a^4/Eh^4 = 2173.4$; Dashed line: $pR_a^4/Eh^4 = 5278.3$.

Table 5: The convergent homotopy-approximation of the load Q in case of different values of a for a circular plate with the simple support boundary, given by the HAM-based 1st-order iteration approach with the truncation order N given by (77) and the optimal convergence-control parameter c_0 given by (80).

a	c_0	N	Q
10	-0.44	100	107.8
20	-0.17	140	737.4
30	-0.08	210	2304.8
40	-0.05	280	5199.8
50	-0.03	350	9799.3

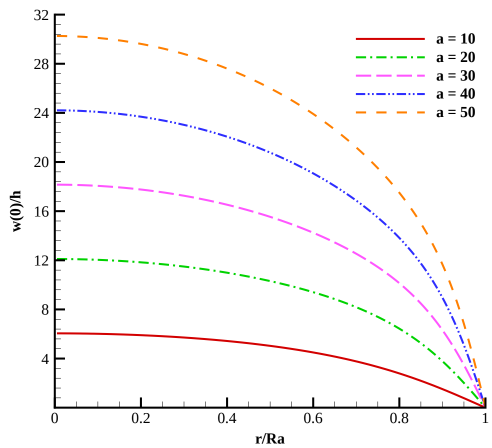

Figure 12: The deflection curves of a thin circular plate with the simple support boundary given by the HAM-based 1st-order iteration approach in the case of $a = 10, 20, 30, 40, 50$. Solid line: $pR_a^4/Eh^4 = 95.6$; Dash-dotted line: $pR_a^4/Eh^4 = 653.9$; Dashed line: $pR_a^4/Eh^4 = 2043.9$; Dash-double-dotted line: $pR_a^4/Eh^4 = 4611.0$; Dashed line: $pR_a^4/Eh^4 = 8689.9$.

Table 6: The convergent homotopy-approximation of the load Q in case of different values of a for a circular plate with the boundary of simple hinged support given by the HAM-based 1st-order iteration approach with the truncation order N given by (77) and the optimal convergence-control parameter c_0 given by (81).

a	c_0	N	Q
10	-0.112	100	890.0
20	-0.021	100	7152.3
30	-0.008	150	24166.4
40	-0.004	200	57308.7
50	-0.002	250	111955.3

ods) and the modified iteration method [4] are only the special cases of the HAM approaches.

Vincent [2] used the load Q as a perturbation quantity to obtain perturbation results that however are valid only for $w(0)/h < 0.52$ in the case of the

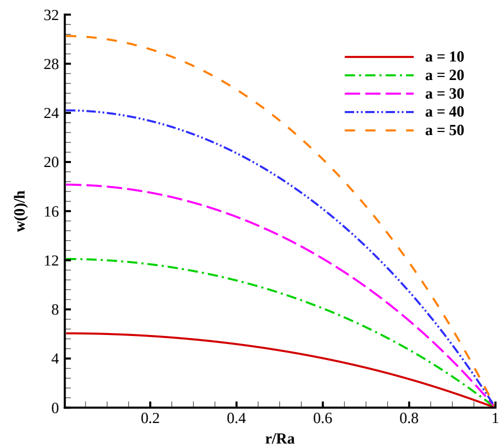

Figure 13: The deflection curves of a thin circular plate with the boundary of simple hinged support given by the HAM-based 1st-order iteration approach in the case of $a = 10, 20, 30, 40, 50$. Solid line: $pR_a^4/Eh^4 = 789.3$; Dash-dotted line: $pR_a^4/Eh^4 = 6342.5$; Long- dashed line: $pR_a^4/Eh^4 = 21430.3$; Dash-double-dotted line: $pR_a^4/Eh^4 = 50820.2$; Dashed line: $pR_a^4/Eh^4 = 99279.8$.

clamped boundary. Chien [3] took $W(0)$ as the perturbation quantity and obtained the convergent results for $w(0)/h < 2.44$ in the case of the clamped boundary. It is very interesting that both of Vincent's [2] and Chien's [3] perturbation methods are special cases of the HAM-based approach in case of $c_0 = -1$, as proved in Appendix A. However, the HAM approach can give convergent results in much larger range of $w(0)/h$ by means of choosing a proper value of the convergence-control parameter c_0. For example, as shown in Fig. 14, the convergent solution can be obtained by means of the HAM-based approach (without iteration) with $c_0 = -0.2$ in the case of $a = 5$, corresponding to $w(0)/h = 3.0$, where Chien's perturbation method [3] is invalid.

The modified iterative method [4] inherits the merits of Chien's perturbation method [3] and iteration technique, but with the computational efficiency much higher than Chien's perturbation method. However, Zhou [20] proved that, if the iterative parameter in the modified iterative method [4] is the same as the perturbation quantity in the perturbation methods, results given by the two methods have the same convergent region. Thus, iteration itself can not modify the convergence! In fact, the modified iterative method [4] is also a special case of the HAM-based 1st-order iteration approach when $c_0 = -1$ (for details, please see Appendix B). However, the HAM iteration approach can give convergent results in much larger range of $w(0)/h$ by means of choosing a proper value of the convergence-control parameter c_0. As shown in Fig. 15, the convergent result can be obtained by means of the HAM-based 1st-order iteration approach with $c_0 = -0.2$ in the case of $a = 10$, equivalent to $w(0)/h = 6.1$, where the modified iterative method [4] is invalid.

Therefore, not only the perturbation methods for any a perturbation quantity (including Vincent's [2] and Chien's [3] perturbation methods) but also the modified iteration method [4] are only the special cases of the HAM (without iteration) and the HAM-based iteration approach when $c_0 = -1$, respectively. More importantly, by means of choosing a proper value of the convergence-control parameter c_0 in the frame of the HAM approach, convergent solutions can be obtained in a much larger region where perturbation methods [2, 3] and the modified iteration method [4] fail, as shown in Fig. 14 and Fig. 15 as examples. Therefore, it is the convergence-control parameter c_0 that guarantees the convergence of solutions for a circular plate under an arbitrary uniform external pressure. This explains why the HAM-based approach can gain convergent results even for quite large load. So, these relations proved in the Appendix A and B indicate the novelty and potential of the HAM once again. Indeed, it is the convergence-control parameter c_0 that differs the HAM from all other approximation methods!

In Part (II), we will prove that even the interpolation iterative method [21] is a special case of the HAM-based iteration approach.

5. Conclusions

In this paper, the homotopy analysis method (HAM) is applied to the large deflection of a circular plate under a uniform external pressure with four different kinds of boundaries. Convergent analytical solutions are successfully obtained, with large enough convergent region ($w(0)/h > 20$) for the majority of applications. It is found that iteration can greatly accelerate the convergence of solutions. In addition, we prove that not only the perturbation methods for any a perturbation quantity (including Vincent's [2] and Chien's [3] perturbation methods) but also the modified iteration method [4] are only the special cases of the HAM (without iteration) and the

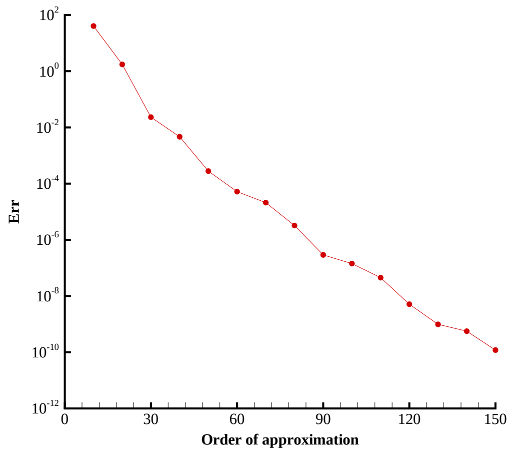

Figure 14: The sum of the squared residual errors Err at different order of approximations in the case of $a = 5$ for a circular plate with the clamped boundary given by the HAM-based approach (without iteration) using $c_0 = -0.2$.

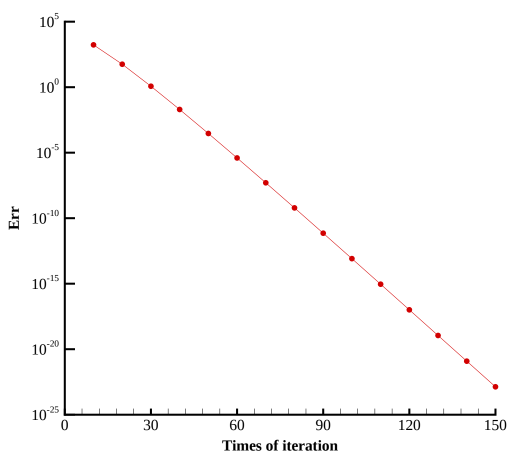

Figure 15: The sum of the squared residual errors Err versus times of iteration in the case of $a = 10$ for a circular plate with the clamped boundary given by the HAM-based 1st-order iteration approach using $c_0 = -0.2$.

HAM-based iteration approach when $c_0 = -1$, respectively[†]. Especially, by choosing a proper value of the convergence-control parameter c_0, convergent solutions can be gained for an *arbitrary* uniform external pressure. Indeed, it is the convergence-control parameter c_0 that provides us with a simple way to greatly enlarge convergent regions, as shown in this paper. Besides, it is also the convergence-control parameter that differs the HAM from all other analytic approximation methods.

This paper indicates the validity of the HAM for the famous Von Kármán plate equation in solid mechanics, and shows the superiority of the HAM over perturbation methods. Without doubt, the HAM can be further applied to solve some challenging nonlinear problems in solid mechanics.

Acknowledgment

This work is partly supported by National Natural Science Foundation of China (Approval No. 11272209 and 11432009) and State Key Laboratory of Ocean Engineering (Approval No. GKZD010063).

Appendix A. Relations between the perturbation methods and the HAM approach

Here we prove that the perturbation methods for any a perturbation quantity (including Vincent's [2] and Chien's [3] perturbation methods) are special cases of a kind of HAM approach when $c_0 = -1$.

First, we describe the perturbation methods for a circular plate under a uniform pressure in a general way. Let ζ denote a perturbation quantity.

[†]In Part (II), we will prove that even the interpolation iterative method [21] is a special case of the HAM-based iteration approach.

Write the perturbation series

$$\begin{aligned}
\varphi^{(P)}(y) &= \sum_{i=1}^{+\infty} \varphi_i^{(P)}(y)\zeta^{2i-1}, &\text{(A-1)}\\
S^{(P)}(y) &= \sum_{i=1}^{+\infty} S_i^{(P)}(y)\zeta^{2i}, &\text{(A-2)}\\
Q^{(P)} &= \sum_{i=1}^{+\infty} Q_i^{(P)}\zeta^{2i-1}, &\text{(A-3)}\\
W^{(P)}(0) &= \sum_{i=1}^{+\infty} W_i^{(P)}(0)\zeta^{2i-1}, &\text{(A-4)}
\end{aligned}$$

with the definition

$$S_0^{(P)}(y) = 0.$$

Substituting Eqs.(A-1)-(A-4) into Eqs.(1)-(4) and (7), and equating the like-power of ζ, we have the governing equation

$$\begin{aligned}
y^2 \frac{d^2\varphi_m^{(P)}(y)}{dy^2} &= \sum_{i=1}^{m} \varphi_i^{(P)}(y) S_{m-i}^{(P)}(y) + Q_m^{(P)} \cdot y^2,\\
y^2 \frac{d^2 S_m^{(P)}(y)}{dy^2} &= -\frac{1}{2}\sum_{i=1}^{m} \varphi_i^{(P)}(y)\varphi_{m+1-i}^{(P)}(y), \qquad \text{(A-5)}
\end{aligned}$$

subject to the boundary conditions

$$\varphi_m^{(P)}(0) = S_m^{(P)}(0) = 0, \qquad \text{(A-6)}$$

$$\varphi_m^{(P)}(1) = \frac{\lambda}{\lambda - 1} \cdot \left.\frac{d\varphi_m^{(P)}(y)}{dy}\right|_{y=1}, \qquad S_m^{(P)}(1) = \frac{\mu}{\mu - 1} \cdot \left.\frac{dS_m^{(P)}(y)}{dy}\right|_{y=1}, \qquad \text{(A-7)}$$

with the restriction condition:

$$-\int_0^1 \frac{1}{\varepsilon} \cdot \varphi_m^{(P)}(\varepsilon) d\varepsilon = W_m^{(P)}(0). \qquad \text{(A-8)}$$

Note that there is an another equation that characterizes the relation between the physical parameter ζ and the central deflection $W(0)$, which can provide an another restriction condition. Thus, the above-mentioned perturbation approach is well defined. Note that this perturbation approach is valid for *arbitrary* physical parameter ζ. So, it is rather general.

The Von Kármán's equation for a circular plate under a uniform pressure can be solved by the HAM in the following way that is a little different from those mentioned in § 2.

Let the initial guesses of $\varphi(y)$, $S(y)$, Q and $W(0)$ be zero, c_0 denote the convergence-control parameter, $\mathcal{L}$ the auxiliary linear operator defined by (61), $H_1(y)$ and $H_2(y)$ the auxiliary functions defined by (65), $q \in [0,1]$ the embedding parameter, respectively. We construct the zeroth-order deformation equation:

$$(1-q)\mathcal{L}[\tilde{\Phi}(y;q)] = c_0\ q\ H_1(y)\ \tilde{\mathcal{N}_1}(y;q), \tag{A-9}$$

$$(1-q)\mathcal{L}[\tilde{\Xi}(y;q)] = c_0\ q\ H_2(y)\ \tilde{\mathcal{N}_2}(y;q), \tag{A-10}$$

subject to the boundary conditions

$$\tilde{\Phi}(0;q) = \tilde{\Xi}(0;q) = 0, \tag{A-11}$$

$$\tilde{\Phi}(1;q) = \frac{\lambda}{\lambda-1}\cdot\left.\frac{\partial\tilde{\Phi}(y;q)}{\partial y}\right|_{y=1}, \quad \tilde{\Xi}(1;q) = \frac{\mu}{\mu-1}\cdot\left.\frac{\partial\tilde{\Xi}(y;q)}{\partial y}\right|_{y=1}, \tag{A-12}$$

with the restriction condition

$$-\int_0^1 \frac{1}{\varepsilon}\tilde{\Phi}(\varepsilon;q)d\varepsilon = \tilde{\Psi}(q), \tag{A-13}$$

where

$$\tilde{\mathcal{N}_1}(y;q) = y^2\frac{d^2\tilde{\Phi}(y;q)}{dy^2} - \left(\frac{1}{q}\right)\tilde{\Phi}(y;q)\tilde{\Xi}(y;q) - \left(\frac{1}{q}\right)\tilde{\Theta}(q)y^2, \tag{A-14}$$

$$\tilde{\mathcal{N}_2}(y;q) = y^2\frac{d^2\tilde{\Xi}(y;q)}{dy^2} + \left(\frac{1}{2q^2}\right)\tilde{\Phi}^2(y;q), \tag{A-15}$$

are two nonlinear operators.

When $q=0$, the solutions of Eqs. (A-9)-(A-13) are the initial guess, i.e.

$$\tilde{\Phi}(y;0) = 0, \quad \tilde{\Xi}(y;0) = 0, \quad \tilde{\Theta}(0) = 0, \quad \tilde{\Psi}(0) = 0. \tag{A-16}$$

When $q=1$, Eqs. (A-9)-(A-13) are equivalent to the original equations (1)-(4) and (31), provided

$$\tilde{\Phi}(y;1) = \varphi(y), \quad \tilde{\Xi}(y;1) = S(y), \quad \tilde{\Theta}(1) = Q, \quad \tilde{\Psi}(1) = W(0). \tag{A-17}$$

Therefore, as q increases from 0 to 1, $\tilde{\Phi}(y;q)$ varies continuously from the initial guess $\varphi_0(y) = 0$ to $\varphi(y)$, so do $\tilde{\Xi}(y;q)$ from the initial guess $S_0(y) = 0$ to $S(y)$, $\tilde{\Theta}(q)$ from 0 to Q, and $\tilde{\Psi}(q)$ from 0 to $W(0)$, respectively.

Expanding $\tilde{\Phi}(y;q)$, $\tilde{\Xi}(y;q)$, $\tilde{\Theta}(q)$ and $\tilde{\Psi}(q)$ into Taylor series with respect to the embedding parameter q and using (A-16), we have the so-called homotopy-series:

$$\tilde{\Phi}(y;q) = \sum_{m=1}^{+\infty} \tilde{\varphi}_m(y)\, q^m, \tag{A-18}$$

$$\tilde{\Xi}(y;q) = \sum_{m=1}^{+\infty} \tilde{S}_m(y)\, q^m, \tag{A-19}$$

$$\tilde{\Theta}(q) = \sum_{m=1}^{+\infty} \tilde{Q}_m\, q^m, \tag{A-20}$$

$$\tilde{\Psi}(q) = \sum_{m=1}^{+\infty} \tilde{W}_m(0)\, q^m. \tag{A-21}$$

Assume that the convergence-control parameter c_0 is properly chosen so that the homotopy-series (A-18)-(A-21) are convergent at $q = 1$. Then, according to Eq. (A-17), we have the homotopy-series solutions:

$$\varphi(y) = \sum_{m=1}^{+\infty} \tilde{\varphi}_m(y), \tag{A-22}$$

$$S(y) = \sum_{m=1}^{+\infty} \tilde{S}_m(y), \tag{A-23}$$

$$Q = \sum_{m=1}^{+\infty} \tilde{Q}_m, \tag{A-24}$$

$$W(0) = \sum_{m=1}^{+\infty} \tilde{W}_m(0). \tag{A-25}$$

Substituting the series (A-18)-(A-21) into the zeroth−order deformation equations (A-9)-(A-13) and then equating the like-power of the embedding parameter q, we have the mth-order deformation equations by means of the definitions (61) and (65):

$$y^2 \frac{d^2}{dy^2}\left[\tilde{\varphi}_m(y) - \chi_m \tilde{\varphi}_{m-1}(y)\right] = c_0\, \tilde{\delta}_{1,m-1}(y), \tag{A-26}$$

$$y^2\frac{d^2}{dy^2}\left[\tilde{S}_m(y)-\chi_m\tilde{S}_{m-1}(y)\right]=c_0\;\tilde{\delta}_{2,m-1}(y), \tag{A-27}$$

subject to the boundary conditions

$$\tilde{\varphi}_m(0)=\tilde{S}_m(0)=0, \tag{A-28}$$

$$\tilde{\varphi}_m(1)=\frac{\lambda}{\lambda-1}\cdot\left.\frac{\partial\tilde{\varphi}_m(y)}{\partial y}\right|_{y=1},\qquad \tilde{S}_m(1)=\frac{\mu}{\mu-1}\cdot\left.\frac{\partial\tilde{S}_m(y)}{\partial y}\right|_{y=1}, \tag{A-29}$$

with the restriction condition:

$$-\int_0^1\frac{1}{\varepsilon}\cdot\tilde{\varphi}_m(\varepsilon)d\varepsilon=\tilde{W}_m(0), \tag{A-30}$$

where χ_m is defined by (22) and

$$\begin{aligned}\tilde{\delta}_{1,m-1}(y) &= \mathcal{D}_{m-1}[\tilde{\mathcal{N}}_1(y;q)]\\ &= y^2\frac{d^2\tilde{\varphi}_{m-1}(y)}{dy^2}-\sum_{i=0}^{m}\tilde{\varphi}_i(y)\tilde{S}_{m-i}(y)-\tilde{Q}_m y^2, \qquad \text{(A-31)}\\ \tilde{\delta}_{2,m-1}(y) &= \mathcal{D}_{m-1}[\tilde{\mathcal{N}}_1(y;q)]\\ &= y^2\frac{d^2\tilde{S}_{m-1}(y)}{dy^2}+\frac{1}{2}\sum_{i=0}^{m}\tilde{\varphi}_i(y)\tilde{\varphi}_{m+1-i}(y). \qquad \text{(A-32)}\end{aligned}$$

Set $c_0=-1$ and write for $m\geq 1$:

$$\begin{aligned}\tilde{\varphi}_m(y) &= \hat{\varphi}_m(y)\,\zeta^{2m-1},\qquad \tilde{S}_m(y)=\hat{S}_m(y)\,\zeta^{2m}, \qquad \text{(A-33)}\\ \tilde{Q}_m &= \hat{Q}_m\,\zeta^{2m-1},\qquad \tilde{W}_m(0)=\hat{W}_m(0)\,\zeta^{2m-1}. \qquad \text{(A-34)}\end{aligned}$$

Substituting Eqs.(A-33)-(A-34) into the m-th deformation equations (A-26)-(A-30) and using (A-16), we have the governing equations ($m\geq 1$):

$$\begin{aligned}y^2\frac{d^2\hat{\varphi}_m(y)}{dy^2} &= \sum_{i=1}^{m}\hat{\varphi}_i(y)\hat{S}_{m-i}(y)+\hat{Q}_m y^2, \qquad \text{(A-35)}\\ y^2\frac{d^2\hat{S}_m(y)}{dy^2} &= -\frac{1}{2}\sum_{i=1}^{m}\hat{\varphi}_i(y)\hat{\varphi}_{m+1-i}(y), \qquad \text{(A-36)}\end{aligned}$$

subject to the boundary conditions

$$\hat{\varphi}_m(0)=\hat{S}_m(0)=0, \tag{A-37}$$

$$\hat{\varphi}_m(1) = \frac{\lambda}{\lambda - 1} \cdot \left. \frac{d\hat{\varphi}_m(y)}{dy} \right|_{y=1}, \qquad \hat{S}_m(1) = \frac{\mu}{\mu - 1} \cdot \left. \frac{d\hat{S}_m(y)}{dy} \right|_{y=1}, \qquad \text{(A-38)}$$

and the restriction condition for $\hat{Q}_m$:

$$-\int_0^1 \frac{1}{\varepsilon} \cdot \hat{\varphi}_m(\varepsilon) d\varepsilon = \hat{W}_m(0). \qquad \text{(A-39)}$$

Note that Eqs.(A-35)-(A-39) are exactly the same as Eqs.(A-5)-(A-8), thus

$$\hat{\varphi}_m(y) = \varphi_m^{(P)}(y), \quad \hat{S}_m(y) = S_m^{(P)}(y), \quad \hat{Q}_m = Q_m^{(P)}, \quad \hat{W}_m(0) = W_m^{(P)}(0).$$

Then we have

$$\begin{aligned}
\varphi^{(P)}(y) &= \sum_{i=1}^{+\infty} \varphi_i^{(P)}(y)\zeta^{2i-1} = \sum_{i=1}^{+\infty} \hat{\varphi}_i(y)\zeta^{2i-1} = \sum_{i=1}^{+\infty} \tilde{\varphi}_i(y) = \varphi(y), \\
S^{(P)}(y) &= \sum_{i=1}^{+\infty} S_i^{(P)}(y)\zeta^{2i-1} = \sum_{i=1}^{+\infty} \hat{S}_i(y)\zeta^{2i-1} = \sum_{i=1}^{+\infty} \tilde{S}_i(y) = S(y), \\
Q^{(P)} &= \sum_{i=1}^{+\infty} Q_i^{(P)}\zeta^{2i-1} = \sum_{i=1}^{+\infty} \hat{Q}_i\zeta^{2i-1} = \sum_{i=1}^{+\infty} \tilde{Q}_i = Q, \\
W^{(P)}(0) &= \sum_{i=1}^{+\infty} W_i^{(P)}(0)\zeta^{2i-1} = \sum_{i=1}^{+\infty} \hat{W}_i(0)\zeta^{2i-1} = \sum_{i=1}^{+\infty} \tilde{W}_i(0) = W(0).
\end{aligned}$$

Therefore, the perturbation methods for *arbitrary* perturbation quantity ζ are only special case of the HAM when $c_0 = -1$.

If we choose the perturbation quantity $\zeta = Q$, Eqs. (A-35)-(A-39) become

$$y^2 \frac{d^2\hat{\varphi}_m(y)}{dy^2} = \sum_{i=1}^{m} \hat{\varphi}_i(y)\hat{S}_{m-i}(y) + (1 - \chi_m)y^2, \qquad \text{(A-40)}$$

$$y^2 \frac{d^2\hat{S}_m(y)}{dy^2} = -\frac{1}{2}\sum_{i=1}^{m} \hat{\varphi}_i(y)\hat{\varphi}_{m+1-i}(y), \qquad \text{(A-41)}$$

subject to the boundary conditions

$$\hat{\varphi}_m(0) = \hat{S}_m(0) = 0, \qquad \text{(A-42)}$$

$$\hat{\varphi}_m(1) = \frac{\lambda}{\lambda - 1} \cdot \left. \frac{d\hat{\varphi}_m(y)}{dy} \right|_{y=1}, \qquad \hat{S}_m(1) = \frac{\mu}{\mu - 1} \cdot \left. \frac{d\hat{S}_m(y)}{dy} \right|_{y=1}. \qquad \text{(A-43)}$$

Note that Eqs. (A-40)-(A-43) are exactly the same as Eqs. (10)-(13) for the Vincent's perturbation method [2].

If we choose the perturbation quantity $\zeta = W(0)$, Eqs.(A-35)-(A-39) become

$$y^2 \frac{d^2 \hat{\varphi}_m(y)}{dy^2} = \sum_{i=1}^{m} \hat{\varphi}_i(y) \hat{S}_{m-i}(y) + \hat{Q}_m y^2, \tag{A-44}$$

$$y^2 \frac{d^2 \hat{S}_m(y)}{dy^2} = -\frac{1}{2} \sum_{i=1}^{m} \hat{\varphi}_i(y) \hat{\varphi}_{m+1-i}(y), \tag{A-45}$$

(A-46)

subject to the boundary conditions

$$\hat{\varphi}_m(0) = \hat{S}_m(0) = 0, \tag{A-47}$$

$$\hat{\varphi}_m(1) = \frac{\lambda}{\lambda - 1} \cdot \left. \frac{d\hat{\varphi}_m(y)}{dy} \right|_{y=1}, \qquad \hat{S}_m(1) = \frac{\mu}{\mu - 1} \cdot \left. \frac{d\hat{S}_m(y)}{dy} \right|_{y=1}, \tag{A-48}$$

and the restriction condition for $\hat{Q}_m$:

$$-\int_0^1 \frac{1}{\varepsilon} \cdot \hat{\varphi}_m(\varepsilon) d\varepsilon = (1 - \chi_m). \tag{A-49}$$

Then Eqs. (A-44)-(A-49) are the same as Eqs. (17)-(21) for the Chien's perturbation method [3].

So, both of the perturbation methods for any a perturbation quantity (including Vincent's [2] and Chien's [3] perturbation methods) are only special cases of the HAM when $c_0 = -1$, as mentioned above. It is found that, unlike perturbation methods, the convergence of solution series given by the HAM approach mentioned in the Appendix A can be guaranteed by properly choosing the convergence-control parameter c_0. Thus, the convergence-control parameter c_0 plays a very important role in the frame of the HAM. Indeed, it is the convergence-control parameter c_0 that differs the HAM from all other analytic approximation methods.

Appendix B Relations between the modified iteration method and the HAM-based iteration approach

Substituting the auxiliary linear operator $\mathcal{L}$ defined by (61) and the auxiliary functions $H_1(y)$ and $H_2(y)$ defined by (65) in Eqs. (52) and (53), we have the first-order deformation equation:

$$y^2\frac{d^2\varphi_1(y)}{dy^2} = c_0\left[y^2\frac{d^2\varphi_0(y)}{dy^2} - \varphi_0(y)S_0(y) - Q_0y^2\right], \tag{B-1}$$

$$y^2\frac{d^2S_1(y)}{dy^2} = c_0\left[y^2\frac{d^2S_0(y)}{dy^2} + \frac{1}{2}\varphi_0^2(y)\right]. \tag{B-2}$$

Let

$$\varphi^*(y) = \varphi_0(y) + \varphi_1(y), \quad S^*(y) = S_0(y) + S_1(y)$$

denote the first-order approximation of $\varphi(y)$ and $S(y)$, respectively. We have the governing equation

$$y^2\frac{d^2\varphi^*(y)}{dy^2} = (1+c_0)y^2\frac{d^2\varphi_0(y)}{dy^2} - c_0\left[\varphi_0(y)S_0(y) + Q_0y^2\right], \tag{B-3}$$

$$y^2\frac{d^2S^*(y)}{dy^2} = (1+c_0)y^2\frac{d^2S_0(y)}{dy^2} - \frac{c_0}{2}\varphi_0^2(y). \tag{B-4}$$

subject to the boundary conditions:

$$\varphi^*(0) = S^*(0) = 0, \tag{B-5}$$

$$\varphi^*(1) = \frac{\lambda}{\lambda-1}\cdot\left.\frac{d\varphi^*(y)}{dy}\right|_{y=1}, \qquad S^*(1) = \frac{\mu}{\mu-1}\cdot\left.\frac{dS^*(y)}{dy}\right|_{y=1}, \tag{B-6}$$

and the restriction condition for Q_0:

$$W(0) = -\int_0^1 \frac{1}{\varepsilon}\varphi^*(\varepsilon)d\varepsilon. \tag{B-7}$$

This provides us the first-order iteration approach from the initial guesses $\varphi_0(y), S_0(y)$ to their first-order approximations $\varphi^*(y), S^*(y)$ and the updated value of Q_0. Note that this iteration approach is dependent upon the so-called convergence-control parameter c_0, which plays an important role in guarantee of convergence of the iteration procedure, as illustrated in § 3.2.

In the special case of $c_0 = -1$, we have

$$y^2\frac{d^2\varphi^*(y)}{dy^2} = \varphi_0(y)S_0(y) + Q_0y^2, \tag{B-8}$$

$$y^2\frac{d^2S^*(y)}{dy^2} = \frac{1}{2}\varphi_0^2(y). \tag{B-9}$$

subject to the boundary conditions:

$$\varphi^*(0) = S^*(0) = 0, \tag{B-10}$$

$$\varphi^*(1) = \frac{\lambda}{\lambda - 1} \cdot \left.\frac{d\varphi^*(y)}{dy}\right|_{y=1}, \qquad S^*(1) = \frac{\mu}{\mu - 1} \cdot \left.\frac{dS^*(y)}{dy}\right|_{y=1}, \tag{B-11}$$

and the restriction condition for Q_0:

$$W(0) = -\int_0^1 \frac{1}{\varepsilon}\varphi^*(\varepsilon)d\varepsilon. \tag{B-12}$$

Assume that φ_0, S_0 are known. We take the following iterative procedure:

(a) Calculate $S^*(y)$ according to Eqs.(B-9)-(B-11).

(b) $S_0(y)$ is replaced by $S^*(y)$ that is used as the new initial guess, i.e. $S_0(y) = S^*(y)$.

(c) Calculate $\varphi^*(y)$ and Q_0 according to Eqs. (B-8), (B-10)-(B-12).

(d) $\varphi_0(y)$ is replaced by $\varphi^*(y)$ that is used as the new initial guess, i.e. $\varphi_0(y) = \varphi^*(y)$.

After each step of iteration, $\varphi^*(y)$ and $S^*(y)$ become the new initial guesses for the next iteration. In the nth times of iteration, we set

$$\Theta_n(y) = \varphi^*(y), \qquad \Upsilon_{n-1}(y) = S^*(y), \qquad F_{n-1} = Q_0.$$

Then, the HAM-based 1st-order iteration approach in case of $c_0 = -1$ mentioned-above is expressed by:

$$y^2 \frac{d^2\Upsilon_{n-1}(y)}{dy^2} = -\frac{1}{2}\Theta_{n-1}^2(y), \tag{B-13}$$

$$y^2 \frac{d^2\Theta_n(y)}{dy^2} = \Theta_{n-1}(y)\Upsilon_{n-1}(y) + F_{n-1}y^2, \tag{B-14}$$

subject to the boundary conditions:

$$\Theta_n(0) = \Upsilon_{n-1}(0) = 0, \tag{B-15}$$

$$\Theta_n(1) = \frac{\lambda}{\lambda-1}\cdot\frac{d\Theta_n(y)}{dy}\bigg|_{y=1}, \quad \Upsilon_{n-1}(1) = \frac{\mu}{\mu-1}\cdot\frac{d\Upsilon_{n-1}(y)}{dy}\bigg|_{y=1}, \tag{B-16}$$

and the restriction condition for F_{n-1}:

$$W(0) = a = -\int_0^1 \frac{1}{\varepsilon}\Theta_n(\varepsilon)d\varepsilon. \tag{B-17}$$

We choose the initial guess:

$$\Theta_0(y) = \frac{-2a}{2\lambda+1}[(\lambda+1)y - y^2]. \tag{B-18}$$

Then Eqs. (B-13)-(B-18) are exactly the same as Eqs. (23)-(28) for the modified iteration method [4]. Thus, the modified iterative method [4] is only a special case of the HAM-based 1st-order iteration approach when $c_0 = -1$.

As shown in § 3.2, the convergence-control parameter c_0 plays an important role in guarantee of iteration convergence. Note that iteration itself can only increase the computational efficiency, but unfortunately has no effect on modifying iteration convergence. As shown in § 3, it is the convergence-control parameter that can guarantee the convergence of iteration. This also explains why our HAM-based approaches for the Von kármán's plate of a circular plate are valid for *arbitrary* uniform external pressure.

References

References

[1] V.K.Theodore, Festigkeits problem in maschinenbau, Encycl. Der math. Wiss 4 (1910) 348–351.

[2] J. J. Vincent, The bending of a thin circular plate, Phil. Mag. 12 (1931) 185–196.

[3] W. Z. Chien, Large deflection of a circular clamped plate under uniform pressure, Chi. J. Phys 7 (1947) 102–113.

[4] K. Yeh, R. Liu, S. L. Li, Q. Qing, Nonlinear stabilities of thin circular shallow shells under actions of axisymmetrical uniformly distributed line loads, J. Lanzhou Univ. (Natural Science). 18 (2) (1965) 10–33.

[5] X. J. Zheng, Large deflection theory of circular thin plate and its application, Jilin Science Technology Press, Jilin, 1990.

[6] A. E. H. Love, The small free vibrations and deformation of a thin elastic shell, Philos. Trans. R. Soc. London, Ser. A 17 (1888) 491–546.

[7] V. Karman, H. shen Tsien, The buckling of spherical shells by external pressure, Journal of the Aeronautical Sciences 7 (1940) 43–50.

[8] S. Way, Bending of circular plate with large deflection, ASME Trans. Appl. Mech 56 (1934) 627–636.

[9] W. Z. Chien, Asymptotic behavior of a thin clamped circular plate under uniform normal pressure at very large deflection, Sci. Rep. Natl. TsingHua Univ 5 (1948) 1–24.

[10] D. A. DaDeppo, R. Schmidt, Moderately large deflections of a loosely clamped circular plate under a uniformly distributed load, Indus. Math 25 (1975) 17–28.

[11] J. G. Simmonds, Axisymmetric solution of the von karman plate equation for poisson's ratio one-third, ASME J. of Appl. Mech 50 (4a) (1983) 897–898.

[12] X. J. Zheng, Y. H. Zhou, Exact solution to large deflection of circular plates under compound loads, Sci. China. 4 (1987) 391–404.

[13] J. J. Zheng, X. Z. Zhou, A new numerical method for axisymmetrical bending of circular plates with large deflection, Key Eng. Mater 353-358 (2007) 2699–2702.

[14] X. J. Zheng, J. S. Lee, On the convergence of the chien's perturbation method for von karman plate equations, Int. J. Eng Sci 33 (1995) 1085–1094.

[15] N. Mahmoud, H. J. Al-Gahtani, Rbf-based meshless method for large deflection of thin plates, Eng. Anal. Bound. Elem 31 (2007) 311–317.

[16] S. L. Chen, J. C. Kuang, The perturbation parameter in the problem of large deflection of clamped circular plates, Appl. Math. and Mech.(English Edition) 2 (1) (1981) 137–154.

[17] W. Z. Chien, K. Y. Yeh, On the large deflection of circular plate, China Sci 10 (3) (1954) 209–236.

[18] H. C. Hu, On the large deflection of a circular plate under combined action of uniformly distributed load and concentrated load at the centre, Phys Sin 10 (4) (1954) 383–392.

[19] A. C. Volmir, Flexible plate and shells, Research and Technology Division, Air Force Flight Dynamics Laboratory, 1967.

[20] Y. H. Zhou, On relations between the modified-iterative method and chien's perturbation solution, Appl. Math. and Mech. 10 (1) (1989) 59–70.

[21] H. B. Keller, E. L. Reiss, Iterative solutions for the non-linear bending of circular plates, Commun. Pur. Appl. Math (1958) 273–292.

[22] X. J. Zheng, Y. H. Zhou, On the convergence of the nonlinear equations of circular plate with interpolation iterative method, Chinese. Sci. A 10 (1988) 1050–1058.

[23] P. P. D. Silva, W. Krauth, Numerical solutions of the von karman equations for a thin plate, Int. J. Mod Phys C 8 (2) (1997) 427–434.

[24] L. Waidemam, W. Venturini, Bem formulation for von karman plates, Eng. Anal. Bound. Elem 33 (2009) 1223–1230.

[25] X. J. Liu, Y. H. Zhou, X. M. Wang, J. Z. Wang, A wavelet method for solving a class of nonlinear boundary value problems, Commun. Nonlinear. Sci 18 (2013) 1939–1948.

[26] X. M. Wang, X. J. Liu, J. Z. Wang, Y. H. Zhou, A wavelet method for bending of circular plate with large deflection, Acta. Mech. Solida. Sin 28 (1) (2015) 83–90.

[27] S. J. Liao, Proposed homotopy analysis techniques for the solution of nonlinear problem, PhD thesis, Shanghai Jiao Tong University (1992).

[28] S. J. Liao, Beyond perturbation: introduction to the homotopy analysis method, CHAPMAN & HALL/CRC, Boca Raton, 2003.

[29] S. Liao, Homotopy analysis Method in Nonlinear Differential Equations, Springer-Verlag, New York, 2011.

[30] S. Liao, Notes on the homotopy analysis method: Some definitions and theorems, Commun. Nonlinear Sci. Numer. Simul. 14 (4) (2009) 983–997.

[31] S. J. Liao, An optimal homotopy-analysis approach for strongly nonlinear differential equations, Commun. Nonlinear Sci. Numer. Simul. 15 (8) (2010) 2003–2016.

[32] S. J. Liao, On the method of directly defining inverse mapping for nonlinear differential equations, Numerical Algorithm(published online with DOI: 10.1007/s11075-015-0077-4).

[33] K. Vajravelu, R. A. V. Gorder, Nonlinear Flow Phenomena and Homotopy Analysis: Fluid Flow and Heat Transfer, Springer, Heidelberg, 2012.

[34] S. Abbasbandy, The application of homotopy analysis method to nonlinear equations arising in heat transfer, Physics Letters A 360 (2006) 109 – 113.

[35] T. Hayat, R. Ellahi, P. D. Ariel, S. Asghar, Homotopy solution for the channel flow of a third grade fluid, Nonlinear Dynamics 45 (2006) 55–64.

[36] R. A. V. Gorder, K. Vajravelu, Analytic and numerical solutions to the lane-emden equation, Physics Letters A 372 (2008) 6060–6065.

[37] S. Liang, D. J. Jeffrey, Approximate solutions to a parameterized sixth order boundary value problem, Computers and Mathematics with Applications 59 (2010) 247–253.

[38] A. R. Ghotbi, M. Omidvar, A. Barari, Infiltration in unsaturated soils – an analytical approach, Computers and Geotechnics 38 (2011) 777 – 782.

[39] C. Nassar, J. F. Revelli, R. J. Bowman, Application of the homotopy analysis method to the poissonboltzmann equation for semiconductor devices, Commun. Nonlinear Sci. Numer. Simulat. 16 (2011) 2501 – 2512.

[40] A. Mastroberardino, Homotopy analysis method applied to electrohydrodynamic flow, Commun. Nonlinear Sci. Numer. Simulat. 16 (2011) 2730–2736.

[41] M. Aureli, A framework for iterative analysis of non-classically damped dynamical systems, J. Sound and Vibration 333 (2014) 6688 – 6705.

[42] J. Sardanyés, C. Rodrigues, C. Januário, N. Martins, G. Gil-Gómez, J. Duarte, Activation of effector immune cells promotes tumor stochastic extinction: A homotopy analysis approach, Appl. Math. Comput. 252 (2015) 484 – 495.

[43] K. Zou, S. Nagarajaiah, An analytical method for analyzing symmetry-breaking bifurcation and period-doubling bifurcation, Commun. Nonlinear Sci. Numer. Simulat. 22 (2015) 780–792.

[44] R. A. V. Gorder, Relation between laneemden solutions and radial solutions to the elliptic heavenly equation on a disk, New Astronomy 37 (2015) 42 – 47.

[45] D. Xu, Z. Lin, S. Liao, M. Stiassnie, On the steady-state fully resonant progressive waves in water of finite depth, J. Fluid Mech. 710 (2012) 379.

[46] Z. Liu, S. Liao, Steady-state resonance of multiple wave interactions in deep water, J. Fluid Mech. 742 (2014) 664–700.

[47] Z. Liu, D. Xu, J. Li, T. Peng, A. Alsaedi, S. Liao, On the existence of steady-state resonant waves in experiments, J. Fluid Mech. 763 (2015) 1–23.

[48] S. J. Liao, D. Xu, M. Stiassnie, On the steady-state nearly resonant waves, J. Fluid Mech. 794 (2016) 175–199.

[49] S. J. Liao, D. L. Xu, Z. Liu, On the Discovery of Steady-state Resonant Water Waves, Vol. 908 of Lecture Notes in Physics, Springer, Heidelberg, 2015, Ch. 3, pp. 43 – 82, edited by Elena Tobisch.